Supplemental Materials

Molecular Biology of the Cell

Nguyen et al.

Supplemental Figures

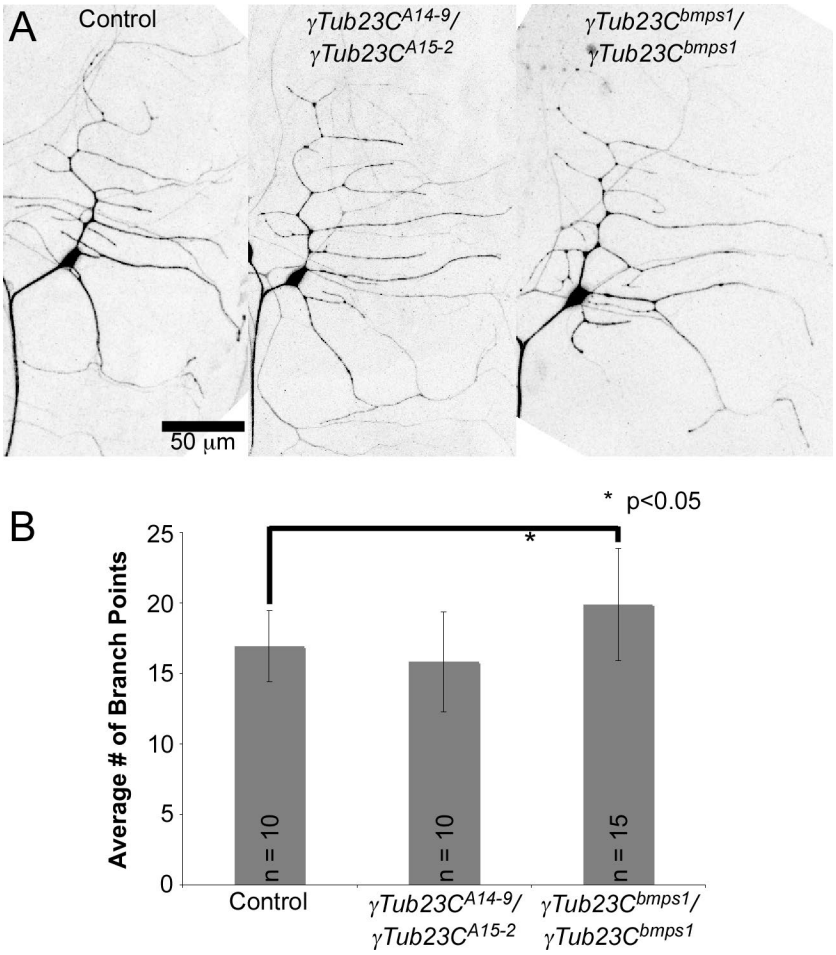

Figure S1. Branching complexity of ddaE dendrite arbors in animals with different alleles of *γ-tubulin*. A. Example images of ddaE neurons in the indicated genetic backgrounds are shown. Overall cell architecture is similar in all cases. **B.** The number of dendrite branch points was counted in entire ddaE dendrite arbors. Averages from the indicated numbers of cells (n) are shown. A t-test was used to calculate statistical significance. Error bars show the standard deviation.

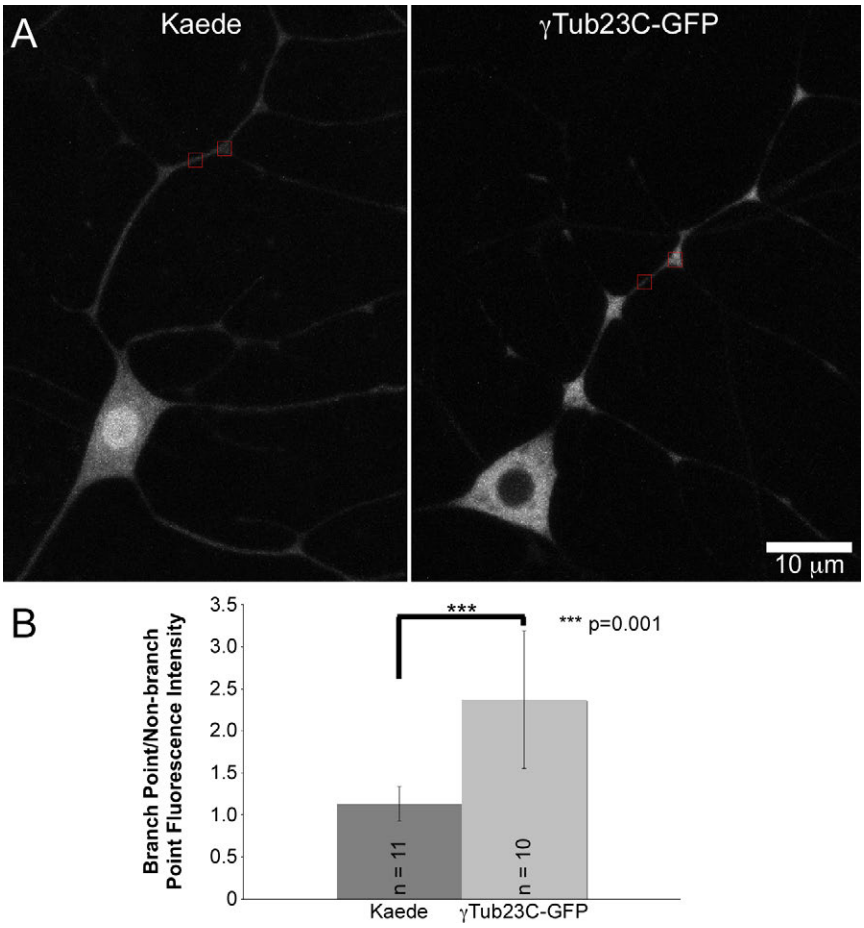

Figure S2. Comparison of a soluble fluorescent protein and γ-tubulin23C-GFP localization in dendrites. To test whether γ-tubulin23C-GFP is specifically concentrated at dendrite branch points, we compared its localization to an untagged soluble fluorescent protein, UAS-Kaede. γ-tubulin23C-GFP and Kaede were expressed in class I neurons with 221-Gal4. **A.** Images of Kaede and γ-tubulin23C-GFP in the ddaE neuron are shown. **B.** The fluorescence intensity of regions inside and between branch points (indicated by small squares) was quantitated using ImageJ, and the ratio was calculated. Error bars show the standard deviation, n's are the number of neurons quantitated, and significance was calculated with a t-test.

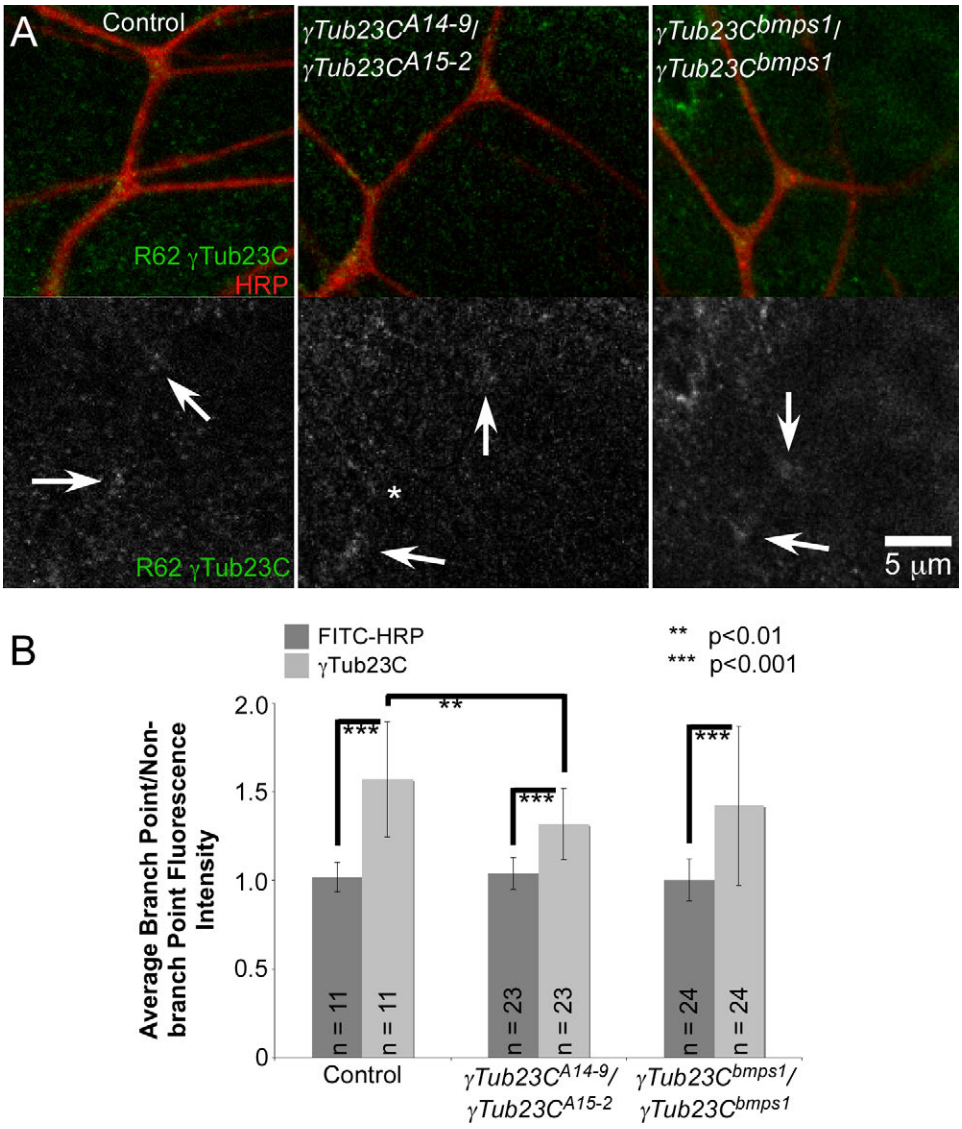

Figure S3. Concentration of endogenous γ-tubulin at dendrite branch points in different *γ-tubulin* mutant backgrounds. A. Examples of γ-tubulin23C staining in ddaE dorsal comb dendrites are shown. Larval filet preps were co-stained with the HRP, which recognizes neuronal membranes in *Drosophila.* Arrows indicate γ-tubulin23C concentrations at branch points. Asterisks indicate less γ-tubulin23C concentrated at branch points. **B.** Ratios of fluorescence at branch point/non-branch point were calculated for both HRP and γ-tubulin staining. Error bars show standard deviations, n's indicate the number of images analyzed, and statistical significance was calculated with a t-test.

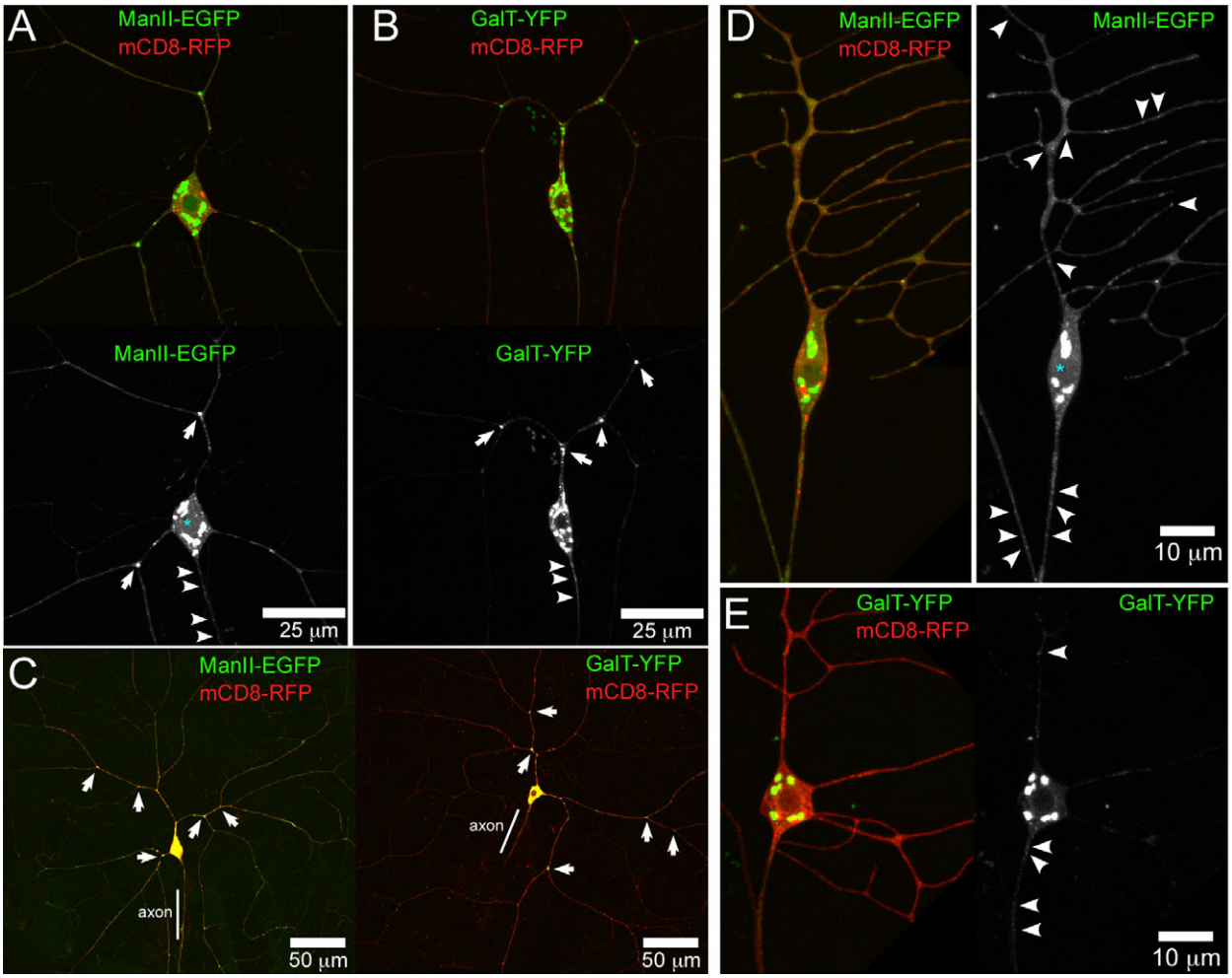

Figure S4. Comparison of GalT-YFP and ManII-eGFP expression in class IV ddaC neurons and class I ddaE neurons. Golgi localization was examined in larval neurons in vivo by expressing mCD8-RFP with GalT-YFP or ManII-eGFP with 477-Gal4 (A-C) or 221-Gal4 (D and E). In all images dorsal is up, and axons emerge from the ventral point on the cell body. **A.** Localization of ManII-eGFP in the ddaC neuron. The ManII signal is shown alone in the lower panel. Clear Golgi outposts are indicated with arrows, and small punctae with arrowheads. The asterisk indicates fluorescent signal in the nucleus. **B.** Localization of GalT-YFP in the ddaC neuron. Golgi outposts are indicated with arrows and small punctae with arrowheads. **C.** Additional examples of Golgi marker localization are shown at lower magnification to give a broader overview of the ddaC cells. **D.** A ddaE neuron expressing ManII-eGFP and mCD8-GFP is shown. Arrowheads point to small punctae in axons and dendrites; dendrites emerge from the top (dorsal) side of the cell body and the axon emerges from the ventral point. An asterisk indicates fluorescence in the nucleus. **E.** GalT-YFP and mCD8-GFP are shown in ddaE. Arrowheads point to very small punctae in axons and dendrites.

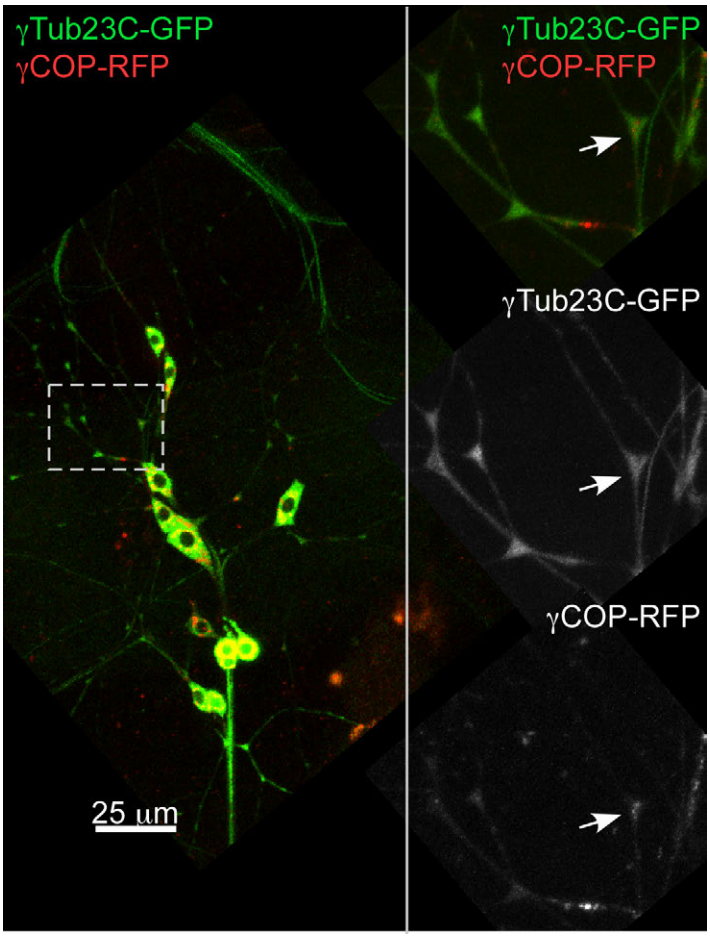

Figure S5. Co-expression of γ-tubulin23C-GFP and γCOP-RFP in *Drosophila* neurons. The pan-neuronal driver elav-Gal4 was used to express γ-tubulin23C-GFP and γCOP-RFP in all *Drosophila* neurons. The overall pattern of γCOP-RFP is similar to the Golgi markers shown in Figure S4. The region in the dotted rectangle is enlarged at the left and a ddaC proximal branch point containing γCOP-RFP spots is indicated with an arrow.

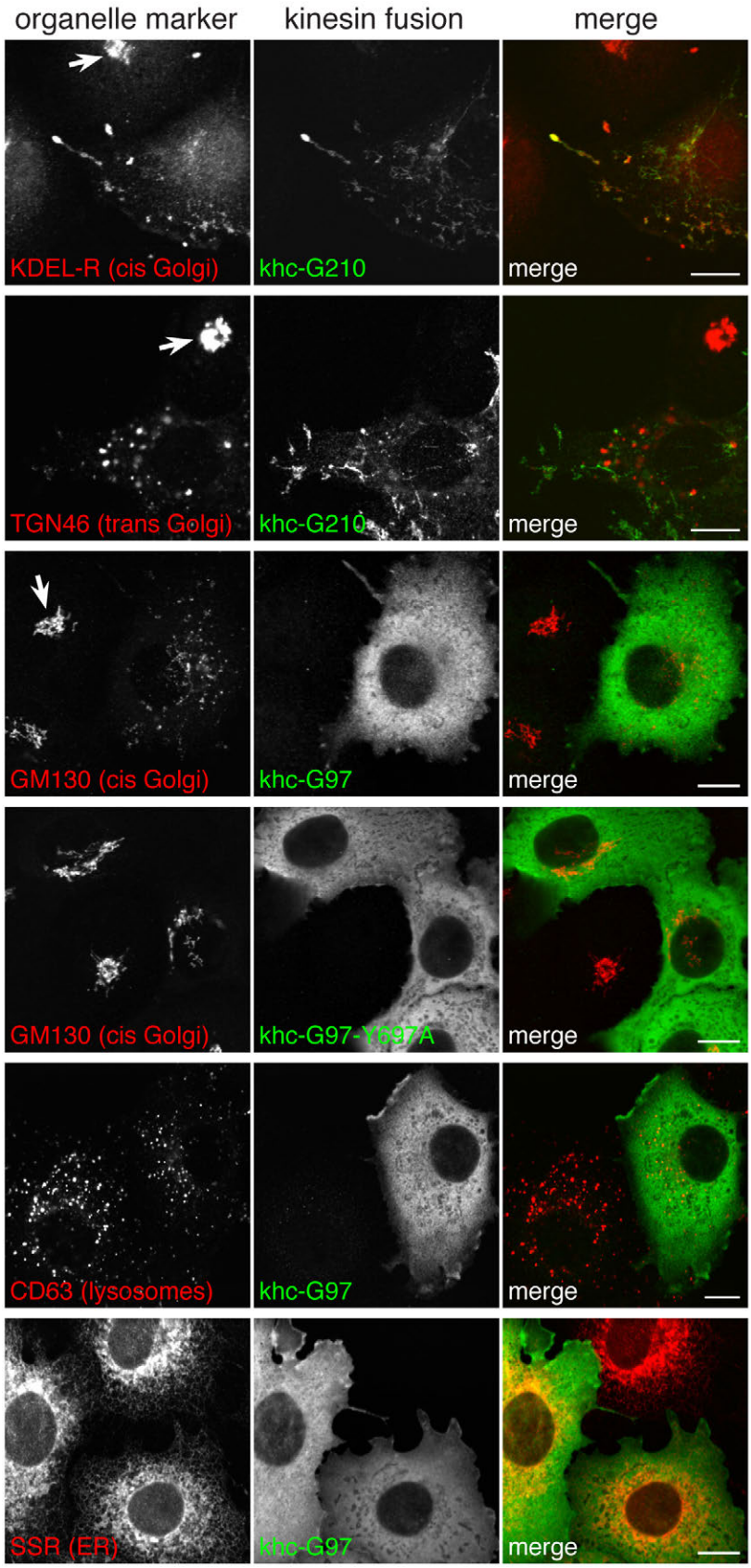

Figure S6. Specific disruption of the Golgi in mammalian cells by Golgi targeted kinesins.

Confocal micrographs of COS cells expressing the indicated kinesin fusions, and immuno-labelled for the myc-tagged kinesin fusion and the indicated organelle markers. The presence of khc-G210 or khc-G97

results in centrifugal scattering of Golgi markers compared to untransfected cells (arrows). Khc-G210 co-localizes with the cis- rather than trans-Golgi derived fragments, consistent with its Golgi targeting domain being from the cis-Golgi protein GMAP-210. The scattering is not simply a consequence of the overexpression of the kinesin motor domain, as it is not seen when the Golgi binding domain contains a mutation that blocks Golgi targeting (khc-G97-Y697A; (Munro and Nichols, 1999)). The distribution of other microtubule-regulated organelles such as lysosomes or ER remains grossly unperturbed. Scale bars 10 μm.

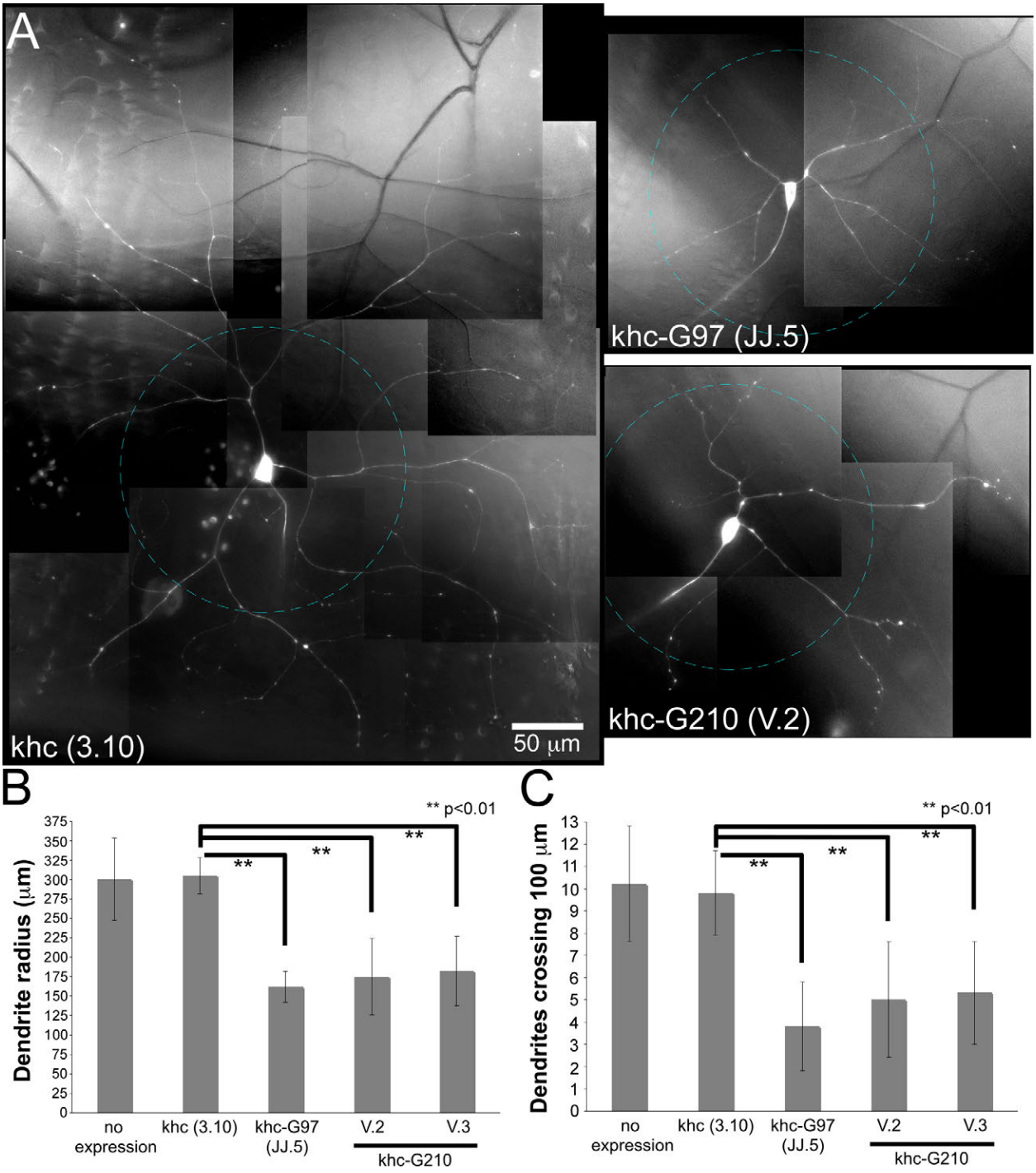

Figure S7. Disruption of the Golgi dramatically reduces the dendrite arbor in both length and complexity in class IV ddaC neurons.

A. Neuronal morphology was examined by expressing EB1-GFP with khc-Golgi fusions using 477-Gal4. Cells expressing the motor domain alone (khc) had normal morphology. Note that with EB1-GFP only large microtubule-containing dendrite branches are visible. **B.** Quantitation of dendrite length was examined by measuring from the center of the soma to the most distal dendrite tip, and the results were then averaged. Error bars represent standard deviations, and a t-test was used to determine significance.

C. Quantitation of dendrite complexity was examined by projecting a circle of a 100 μm radius centered on the cell body onto the image (seen in blue). The number of dendrite branches that cross the circle were then quantified and averaged. Error bars represent standard deviations, and t-test was used to determine significance. Images were acquired with a wide-field microscope and so have more background than is seen in other figures.

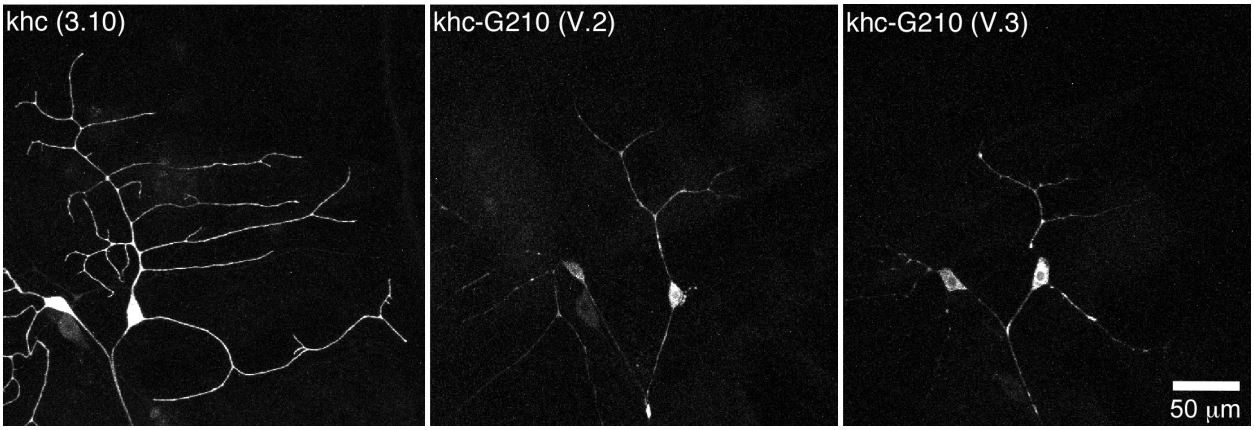

Figure S8. Disruption of the Golgi dramatically reduces the dendrite arbor of class I ddaE neurons. Neuronal morphology was examined by expressing mCD8-RFP using 221-Gal4. Neurons expressing khc-Golgi fusions have much simpler dendrite arbors compared to control neurons that express the fusion without a Golgi-binding domain (khc). Example images are shown.

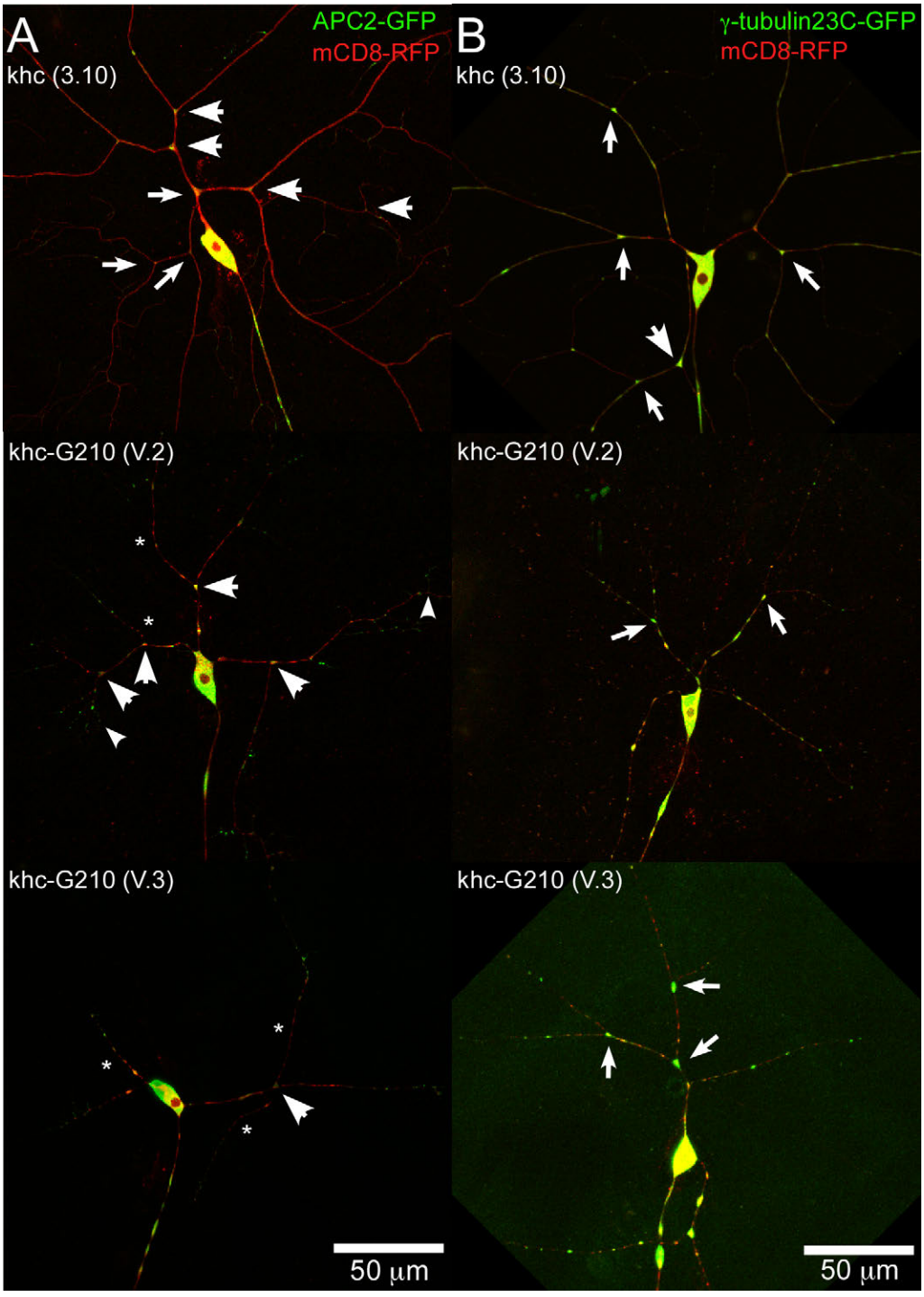

Figure S9. Localization of Apc2-GFP and γ-tubulin23C-GFP in ddaC neurons expressing kinesin-Golgi fusions.

A. Apc2-GFP was expressed with mCD8-RFP and either a control kinesin motor domain or a kinesin-Golgi fusion with 477-Gal4. Representative images of the ddaC neuron are shown. Arrows indicate sites of APC2-GFP localization. Asterisks indicate sites of mCD8-RFP beading. **B.** γ-tubulin23C-GFP was expressed with mCD8-RFP and the kinesin or kinesin-Golgi fusion. Example images of ddaC are shown; arrows indicate branch points with spots of γ-tubulin23C-GFP fluorescence.